Detection of Electrophysiology Catheters in Noisy Fluoroscopy Images

Erik Franken[1], Peter Rongen[2], Markus van Almsick[1], and Bart ter Haar Romeny[1]

[1] Technische Universiteit Eindhoven, Department of Biomedical Engineering, P.O. Box 513, 5600 MB Eindhoven, The Netherlands
{E.M.Franken, M.v.Almsick, B.M.terHaarRomeny}@tue.nl
[2] Philips Medical Systems, Best, The Netherlands
peter.rongen@philips.com

Abstract. Cardiac catheter ablation is a minimally invasive medical procedure to treat patients with heart rhythm disorders. It is useful to know the positions of the catheters and electrodes during the intervention, e.g. for the automatization of cardiac mapping. Our goal is therefore to develop a robust image analysis method that can detect the catheters in X-ray fluoroscopy images. Our method uses steerable tensor voting in combination with a catheter-specific multi-step extraction algorithm. The evaluation on clinical fluoroscopy images shows that especially the extraction of the catheter tip is successful and that the use of tensor voting accounts for a large increase in performance.

1 Introduction

Cardiac catheter ablation is a procedure to treat heart rhythm disorders (arrhythmias). It involves the insertion of one or more flexible thin tubes, called *electrophysiology (EP) catheters*, through small skin incisions, usually in the groin. These catheters are threaded through blood vessels into the heart. The EP catheters contain a number of electrodes used to make *intracardiac electrograms*. Using these electrograms, the firing spot or conduction path causing the arrhythmias can be identified. A special EP catheter (the *ablation catheter*) emits radiofrequency energy to destroy the spot or to block the undesired conduction path. The movement of the catheter through the body is guided using a real-time X-ray fluoroscopy imaging system (Figure 1a).

Catheter ablation is a time-consuming medical procedure, therefore tools to speed up the process are of great interest. An important tool is the automatization of cardiac mapping, i.e. creating a 3D map of cardiac activation patterns over the entire heart. By using bi-plane fluoroscopy, the 3D position of the catheters can be estimated and can be used to superimpose the cardiac activation sequences onto fluoroscopic images. Different research groups and companies are working on this problem, see e.g. [1,2,3]. In these papers, segmentation of the catheters, and especially the electrodes, is considered an important but difficult task to automate. Kynot et al. [1] have proposed an algorithm

R. Larsen, M. Nielsen, and J. Sporring (Eds.): MICCAI 2006, LNCS 4191, pp. 25–32, 2006.

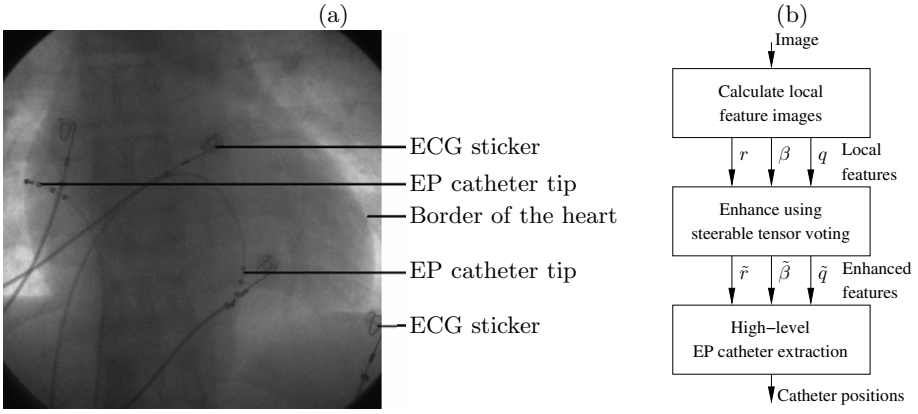

Fig. 1. (a) An example of a typical EP X-ray fluoroscopy image acquired during a clinical intervention. We only want to detect the EP catheters, not the other visible elongated structures. (b) Framework of our method. See text for details.

to detect the electrodes of the catheters, but problems remain in associating the electrodes with the catheters in the image. De Buck et al. [3] constructed an advanced cardiac mapping system, but still require the user to perform a manual segmentation of the catheter and the electrodes. Fallavollita et al. [2] developed a catheter tip detection algorithm based on thresholding of the X-ray image, but due to the noisy nature of fluoroscopy images, the performance is not satisfactory.

In our present work we propose a method for automatic detection of EP catheters in noisy X-ray fluoroscopy images, without the need for any user intervention. Our method detects the catheter bodies as well as the corresponding electrodes. We restrict ourselves to the detection of catheters in a still image, i.e. only spatial information is used.

Figure 1b shows the general framework of our EP catheter extraction process. The method is divided into three main stages. In the first stage, *calculate local feature images*, we perform preprocessing and use local filtering operations to calculate a number of *local feature images*. Because fluoroscopy images are noisy, these local feature images are unreliable. Therefore, the idea behind the next step is to use information from a larger spatial neighborhood, compared to the neighborhood of the local filters, to make the feature images more consistent and specifically enhance the elongated structures. For that purpose we use *steerable tensor voting* [4], which is based on *tensor voting* [5]. In the last stage, *high-level EP catheter extraction*, the enhanced feature images generated by the previous step are used to finally decide where the EP catheters are located. EP catheter-specific properties are used to discriminate the catheters from other line structures.

These three stages will be explained in the next sections. The paper will conclude with an evaluation on clinical images and a discussion.

2 Local Feature Detection

Prior to any filtering we first apply background equalization to remove disturbing structures in the background. We apply a morphological closing operation with a disc-shaped structure element on a slightly blurred version of the input image, to get an image that only contains background structures. Each pixel of the original image is divided by the corresponding pixel in this image to cancel out the background structures.

The second order differential structure of an image gives important information about line-like and blob-like structures. Therefore, we construct a Hessian matrix for each pixel position by calculating second order Gaussian derivatives, see e.g.[6]. We use the 2 eigenvalues λ_1 and λ_2 with $\lambda_1 > \lambda_2$ and corresponding eigenvectors $\mathbf{e}_1$ and $\mathbf{e}_2$ to obtain the following feature images

- A local *ridgeness* image $s(x, y) = \max(\lambda_1(x, y), 0)$, indicating the likelihood that the image contains a line segment at position (x, y). We use λ_1 because its value exactly corresponds to the value one would find when seeking the maximum response of the second order derivative applied in all different orientations. We only keep positive values because we know that catheters are always dark relative to the background.
- A local *orientation* image $\beta(x, y) = \angle\mathbf{e}_1(x, y)$ (where "$\angle$" denotes the angle of the eigenvector relative to the horizontal direction), indicating the most likely orientation of a line segment at position (x, y). The orientation of the first eigenvector corresponds to the orientation at which the response of the second order derivative is maximum.
- A local *blobness* image $q(x, y) = \max(\lambda_2(x, y), 0)$, indicating the likelihood that the image contains a blob-like structure at position (x, y). The motivation is that $\lambda_2 > 0$ implies that $\lambda_1 > \lambda_2 > 0$, which corresponds to a locally concave shape.

3 Contextual Enhancement by Steerable Tensor Voting

To enhance the noisy local ridgeness and orientation measures, we need a model for the continuation of curves in images. For tensor voting [5] we need a function $w(\mathbf{x})$ that indicates the probability that a certain curve passes through position $\mathbf{x}$, given that the same curve passes the origin $(0, 0)$ horizontally. In addition we want to know the most probable angle $\gamma(\mathbf{x})$ of this curve at position $\mathbf{x}$. Different choices are possible for w and γ [4]. In this work, we base the choice on the Gestalt principles [7] of *proximity* (closer curve segments are more likely to belong together) and *good-continuation* (low curvature is favored over large curvature), and get the following functions

$$w(\mathbf{x}) = e^{-\frac{r^2}{2\sigma_{\text{ctx}}^2}} \cos^{2\nu}\phi \text{ and } \gamma(\mathbf{x}) = 2\phi, \quad \text{with } \mathbf{x} = (r\cos\phi, r\sin\phi) \tag{1}$$

where $\sigma_{\text{ctx}} > 0$ is the scale (size) of the function (i.e. this parameter controls the proximity), and $\nu \in \mathbb{N}$ determines the angular specificity of the function

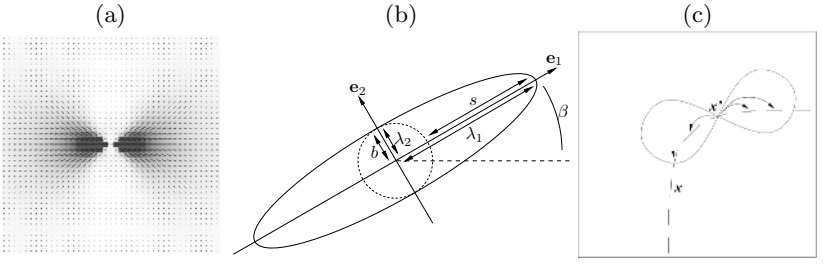

Fig. 2. (a) Example of a stick voting field. Gray scale indicates the value of $w(\mathbf{x})$ (darker means higher value) and the line segments indicate the orientation $\gamma(\mathbf{x})$. (b) Graphical representation of a second rank symmetric semi-positive definite tensor. (c) Illustration of tensor voting illustrated for a single voter at position $\mathbf{x}'$, which broadcasts a vote to its neighbors.

(i.e. this parameter controls the good-continuation). The function for γ expresses the cocircularity constraint, meaning that the most likely connections between two points (with one orientation imposed) is assumed to be a circular arc. The model is visualized in Figure 2a.

In tensor voting, w and γ are combined to generate a tensorial filter kernel $\mathbf{V} : \mathbb{R}^2 \rightarrow \mathbb{R}^2 \times \mathbb{R}^2$ (i.e. a function that assigns a 2×2 matrix to all spatial positions), called the *stick voting field*, as follows

$$\mathbf{V}(\mathbf{x}) = w(\mathbf{x})\, \mathbf{c}(\mathbf{x})\, \mathbf{c}(\mathbf{x})^{\mathrm{T}} \quad \text{with } \mathbf{c}(\mathbf{x}) = \begin{pmatrix} \cos\gamma(\mathbf{x}) \\ \sin\gamma(\mathbf{x}) \end{pmatrix}. \tag{2}$$

Notice that due to this construction all matrices $\mathbf{V}(\mathbf{x})$ have a largest eigenvalue $\lambda_1(\mathbf{x}) = w(\mathbf{x})$, and the other eigenvalue $\lambda_2(\mathbf{x}) = 0$.

The input for tensor voting is the local ridgeness image s and orientation image β and the output of the method is a tensor field. The operation is intuitively displayed in Figure 2c. The operational definition is

$$\mathbf{U}(\mathbf{x}) = \int_{\Omega} s(\mathbf{x}')\, \mathbf{V}^{\beta(\mathbf{x}')}(\mathbf{x} - \mathbf{x}')\, d\mathbf{x}', \tag{3}$$

where $\mathbf{V}^{\beta}(\mathbf{x})$ is the tensorial voting field rotated over β where rotation is achieved as follows

$$\mathbf{V}^{\beta}(\mathbf{x}) = \mathbf{R}_{\beta}\mathbf{V}(\mathbf{R}_{\beta}^{-1}\mathbf{x})\mathbf{R}_{\beta}^{-1}, \quad \mathbf{R}_{\beta} = \begin{pmatrix} \cos\beta & -\sin\beta \\ \sin\beta & \cos\beta \end{pmatrix}. \tag{4}$$

Since $s(\mathbf{x}) > 0\ \forall \mathbf{x} \in \Omega$, cf. the definition in the previous section, and due to the way $\mathbf{V}$ is constructed, cf. (2), all tensors in the resulting tensor field $\mathbf{U}$ are positive semi-definite and symmetric. From the eigenvalues $\tilde{\lambda}_1, \tilde{\lambda}_2$ and eigenvectors $\tilde{\mathbf{e}}_1, \tilde{\mathbf{e}}_2$ of these tensors we calculate enhanced feature images $\tilde{s}$, $\tilde{\beta}$, and $\tilde{q}$, as follows (omitting spatial coordinates for simplicity)

$$\tilde{s} = \tilde{\lambda}_1 - \tilde{\lambda}_2, \qquad \tilde{\beta} = \angle\tilde{\mathbf{e}}_1, \qquad \tilde{q} = q \cdot (\tilde{\lambda}_1 - \tilde{\lambda}_2). \tag{5}$$

In tensor voting terminology, $\tilde{s}$ is referred to as *stickness* and is a measure for orientation *certainty*, see Figure 2b.

In the EP catheter detection algorithm, we perform two subsequent tensor voting steps. The first one is performed on the local feature images s and β. The enhancement is not always sufficient. To get more consistent curves, directional non-maximum suppression (thinning) is applied on the resulting stickness image to keep the centerlines of the curves, followed by a second tensor voting step with the thinned image as input.

Equation (3) is not straightforward to implement in an efficient way, due to the necessity to constantly rotate the voting field $\mathbf{V}$. Therefore we developed a generic method called *steerable tensor voting* [4]. The idea is to write the tensorial voting field as a *steerable filter* [8] which allows us to implement eq. (3) simply as a sum of a number of complex-valued convolutions, allowing a reduction of complexity from $O(n^4)$ to $O(n^2 \log n)$ where n is the number of pixels in one dimension. This algorithm is might also be very suitable to implement on graphical processing unit (GPU).

4 High-Level Extraction of the EP Catheters

In the last part of the algorithm, we use specific knowledge about EP-catheters to extract them. We will explain it briefly here, and refer to Figure 3a for a schematic overview.

The algorithm consists of three modules. The first module is *path extraction*. The ridgeness and orientation images $\tilde{s}$ and $\tilde{\beta}$ are used to perform directional non-maximum suppression, resulting in an image with curves of 1 pixel thickness. From this image we extract a number of most salient connected pixel strings (the paths). If a path exhibits very high curvature or is likely to be part of branching lines, the path is split to allow proper reconnection in the subsequent steps. From the resulting paths, a *path graph* is created, which has connections between paths whose spatial positions and orientations make it probable that they belong to the same global elongated object in the image.

The second module is *electrode extraction and grouping*. From the blobness image $\tilde{q}$ the most salient local maxima are extracted as electrode candidates. Using the extracted paths and knowledge of typical distances between electrodes, a graph is created with connections between all candidates that might be neighboring electrodes on a catheter. Then, we scan for groups of connected electrodes in this graph that have the best match with the known properties of electrode spacing on EP catheters. These electrode groups and the extracted paths are used to create *catheter tip paths*, describing the curves in the image that connect all electrodes of a catheter with each other.

The catheter tip is now fully extracted (which might already be enough for most applications), but in the third module, *path grouping*, our algorithm also attempts to extract the entire catheter. Using the catheter tips and the path graph, different reasonable extensions of the catheter are considered. The best extension is selected based on a global criterion involving minimization of curvature and change of curvature.

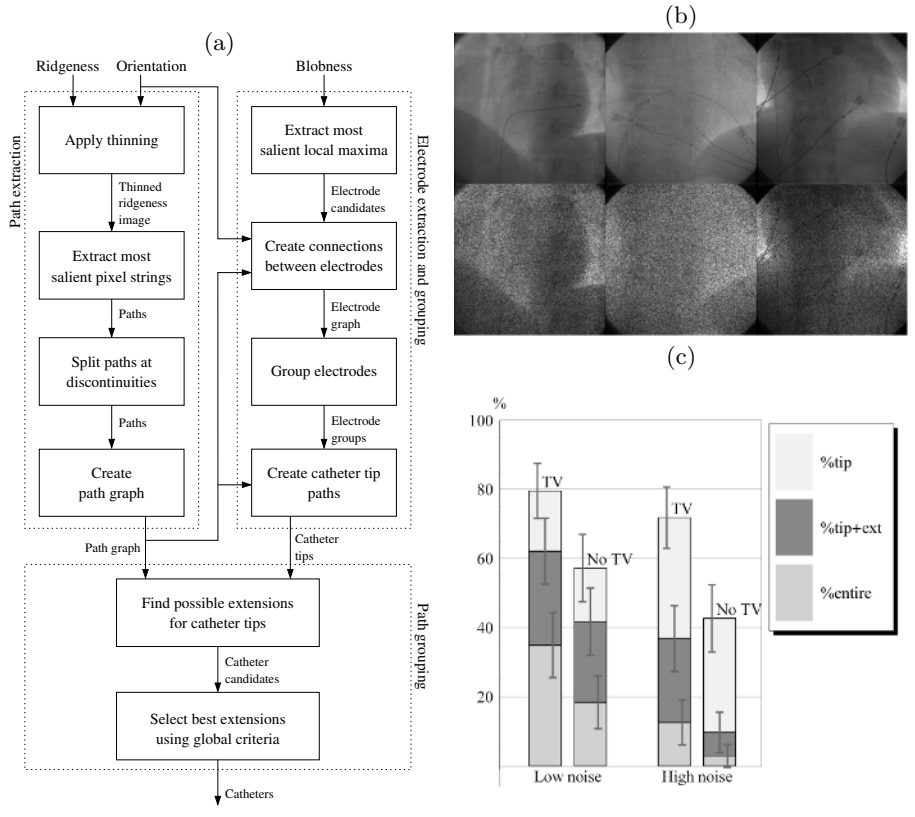

Fig. 3. (a) Schematic overview of the high-level extraction method. (b) three example images from the clinical the test set. Upper row: without additional noise. Lower row: with artificially added multiplicative Poisson noise, which is added to investigate the noise robustness. (c) Extraction results on the test set for low noise and high noise images, and with and without tensor voting. The colours indicate extracted catheter tips (%tip), extracted additional catheter segments (%tip+ext), and extracted entire catheters (% entire). The grey vertical lines with horizontal serifs indicate confidence intervals of 95%.

5 Results

We implemented the EP catheter extraction algorithm partly in Mathematica and partly in C++. The parameters for local feature detection and tensor voting were optimized on 6 different images using the *signal-to-background ratio* as criterion. The parameter values are (512×512 pixel images): scale of Gaussian derivatives $\sigma_{\text{local}} = 3.4$ pixels, angular specificity of the voting field $\nu = 4$, scale of the voting field $\sigma_{\text{ctx}} = 15$ pixels, and scale of the voting field for the second tensor voting step $\sigma_{\text{ctx2}} = 7.5$ pixels. The parameter of the high-level extraction part were optimized using a test set of 10 images. Since these test sets are small, we think that the parameters can be further optimized.

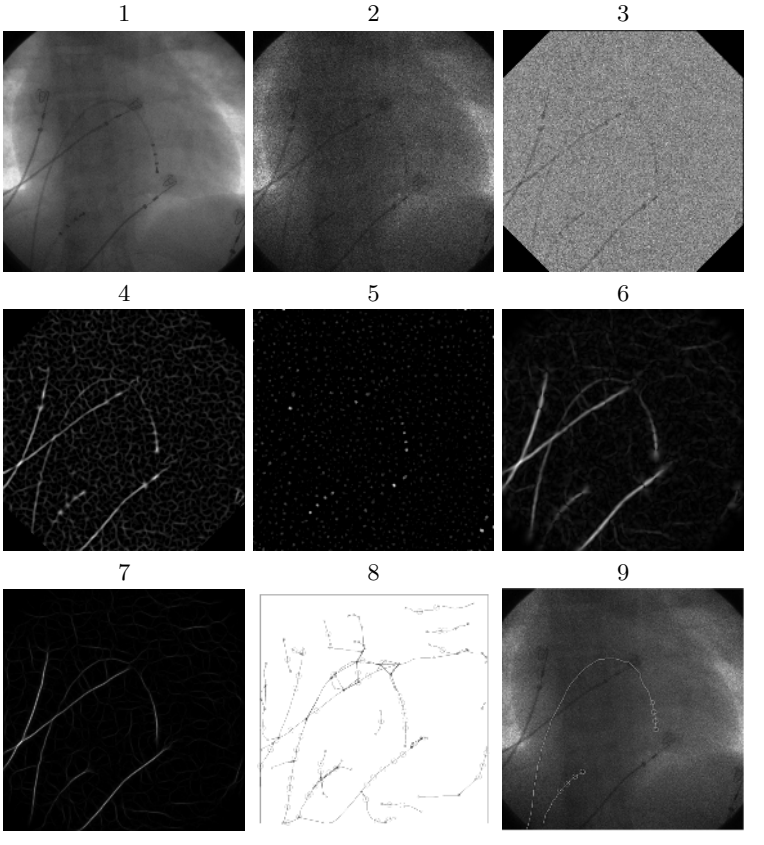

Fig. 4. EP catheter extraction example. 1 - Original image. 2 - Original image with additional noise, used as input for this example. 3 - Background equalized image. 4 - Local ridgeness image. 5 - Blobness image. 6 - Result of first *tensor voting* step. 7 - Result of a second tensor voting step. 8 - Extracted paths and electrode candidates. 9 - Final extraction result.

We used an evaluation set of 50 randomly selected X-ray images acquired during 4 clinical interventions (see Figure 3b), without any image that was used for parameter tuning. These images contain 103 EP catheters that all contain from 4 up to 10 electrodes. The catheters were extracted both with tensor voting and without tensor voting (by simply skipping this step) and both with and without added multiplicative Poisson noise.

Each catheter extraction result was assigned to one of the following categories: (1) catheter not detected at all, (2) successful extraction of the tip only, i.e. the part containing the electrodes, (3) successful extraction of the tip plus an additional catheter segment with the same length, and (4) successful extraction of the entire catheter.

Figure 3c displays the results of the catheter extraction, showing that especially the tip detection is successful. The increase in performance due to tensor

voting is high. For example, the success rate of catheter tip extraction increased from 57% to 80% and from 43% to 72% for low and high noise images respectively. The success rates on extraction of tip+extension and extraction of the entire catheter are still low, especially in noisy images. For clinical practice, however, tip extraction is most relevant. Figure 4 shows an example of the entire EP catheter extraction algorithm.

6 Discussion

We introduced an algorithm for the extraction of EP catheters in fluoroscopy images. One novelty of this work is that we are able to extract the EP catheter fully automatically, without an initial seed, by using an advanced EP catheter-specific high-level extraction algorithm. A further novelty is the use of steerable tensor voting to contextually enhance our image information, thus creating more noise robustness, as shown in the evaluation.

The implementation is currently still too slow for clinical use. The algorithm can, however, be implemented more efficiently. This is an important area of future research. Finally, it should also be noted that both the extraction results and the computational performance could be greatly improved by including the information from previous frames in the image sequence.

References

1. Kynor, D.B., Dietz, A.J., Friets, E.M., Peterson, J.N., Bergstrom, U.C., Triedman, J.K., Hammer, P.E.: Visualization of cardiac wavefronts using data fusion. In Sonka, M., ed.: Medical imaging 2002: Image Processing. Proceedings of the SPIE. Volume 4684., SPIE-Int. Soc. Opt. Eng (2002) 1186–1194
2. Fallavollita, P., Savard, P., Sierra, G.: Fluoroscopic navigation to guide RF catheter ablation of cardiac arrhythmias. In: 26th Annual International Conference of the Engineering in Medicine and Biology Society. (2004)
3. De Buck, S., Maes, F., Ector, J., Bogaert, J., Dymarkowski, S., Heidbchel, H., Suetens, P.: An augmented reality system for patient-specific guidance of cardiac catheter ablation procedures. IEEE Transactions on Medical Imaging, Vol. 24, No. 11, November 2005 **24** (2005) 1512–1524
4. Franken, E., van Almsick, M., Rongen, P., Florack, L., ter Haar Romeny, B.: An efficient method for tensor voting using steerable filters. In: ECCV 2006. (2006) 228–240
5. Medioni, G., Lee, M.S., Tang, C.K.: A Computational Framework for Segmentation and Grouping. Elsevier (2000)
6. ter Haar Romeny, B.M.: Front-end vision vision and multi-scale image analysis. Kluwer Academic Publishers (2003)
7. Wertheimer, M.: Untersuchungen zur Lehre von der Gestalt II. Psychologische Forschung (1923) 301–350
8. Freeman, W.T., Adelson, E.H.: The design and use of steerable filters. IEEE Trans. Pattern Analysis and Machine Intelligence **13** (1991) 891–906